*32nd EPS Conference on Plasma Phys. Tarragona, 27 June - 1 July 2005 ECA Vol.**29C**, P-1.050 (2005)*

Reconstruction of Hydrogenic Ion Temperature Profiles on TCV

Ch. Schlatter, B. P. Duval, A. N. Karpushov

Ecole Polytechnique Fédérale de Lausanne (EPFL),

Centre de Recherches en Physique des Plasmas, CH-1015 Lausanne, Switzerland

Introduction

Using simulated neutral profiles we unfold the energy spectrum of the (line-integrated) neutral hydrogen and deuterium flux measured by TCV's Compact NPA (CNPA, [1]) along the line of sight of the diagnostic, by relating the CNPA ion temperature to a restricted range of the plasma radius, corresponding to where the temperature has been inferred. Together with pseudo chord measurements (vertical displacements of the plasma across the horizontal CNPA view line, figure 1) this procedure is used to reconstruct a CNPA ion temperature profile for $\rho \approx 0.4$ .. 0.9, as shown in figure 2.

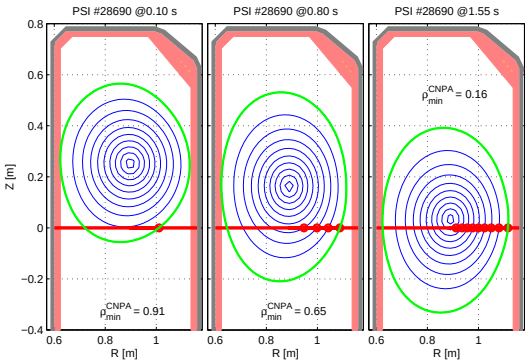

Figure 1: Magnetic topology shown with the horizontal CNPA line of sight at the midplane for a plasma moving downwards at t = 100, 800 and 1550 ms.

Charge exchange spectrum and CNPA temperature

The CNPA measures the energy spectrum of neutrals escaping the plasma. These neutrals contain information about the ion temperature from the diagnosed plasma region. From the measured neutral particle flux F_{CX}^{CNPA} the charge exchange spectrum $\frac{F_{CX}^{CNPA}}{\sigma_{CX}E}$ is commonly shown as function of the energy E (figure 3), from which an effective CNPA ion temperature is obtained using

$$T_i^{CNPA}(E) \approx -\left(\frac{d}{dE}\ln\left|\frac{F_{CX}^{CNPA}}{\sigma_{CX}E}\right|\right)^{-1} \qquad (1)$$

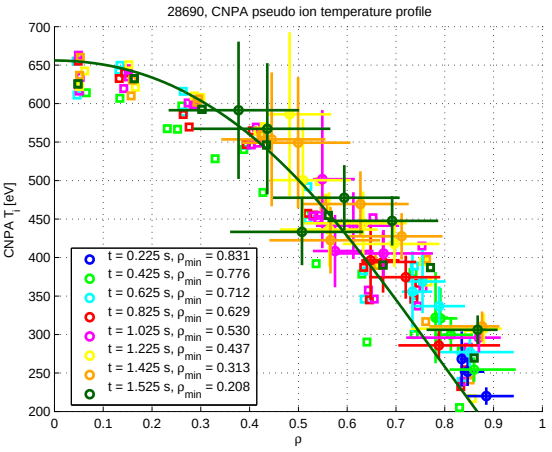

Figure 2: Reconstructed CNPA deuterium T_D ion temperature profile (⊙) and CXRS carbon T_C (measurement □, — fit for t = 1.525 s).

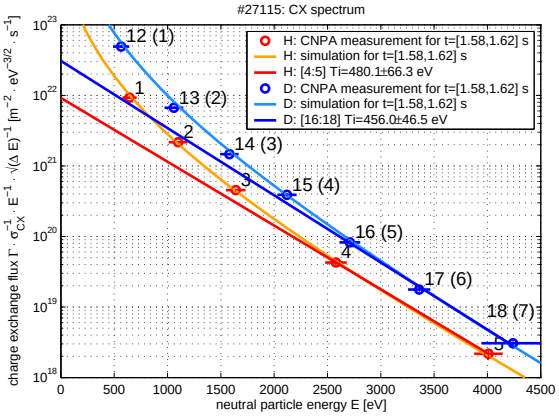

Figure 3: CNPA charge exchange spectrum with temperature fits to channels 4 & 5 and 16-18 for hydrogen and deuterium respectively.

Equation 1 (figure 3) increases with the neutral particle energy, since the more energetic neutrals come from hotter plasma regions. Moving the plasma across the CNPA view line showed that the plasma edge (from LCFS to CNPA) does not influence the spectrum. As described later, neutral particles of a particular energy originate from all plasma radii with a maxwellian energy distribution. The radial position at which the detection energy of the CNPA detector coincides with the maximum of the local energy distribution (determined by T_i) dominates the neutral emission at this energy. Line integrated CNPA measurements alone cannot, however, resolve the place of birth of the detected neutrals. The local neutral birth rate is dominated by charge exchange of hot ions (n_i) on neutrals (n_0). Neutrals may be re-ionised as they travel towards the plasma edge (plasma neutral transparency γ) by electron, ion impact or another charge exchange collision. The emissivity profile $\varepsilon(\rho,E)$ describes the escaping neutrals defined as:

$$\varepsilon(\rho,E) = \gamma(\rho,E)\, f_i(E)\sigma_{CX}(E)v_i(E)n_i(\rho)n_0(\rho) \qquad (2)$$

The electron density n_e and temperature T_e profiles are obtained from Thomson scattering, T_i from Charge eXchange Recombination Spectroscopy (CXRS), n_i is fixed by charge neutrality, v_i by the detector channel energy and f_i by T_i, assuming a maxwellian distribution function. The remaining unknown of equation 2 is the atomic neutral density profile $n_0(\rho)$ for hydrogen and deuterium for the ion neutralisation. To recover the birth place of the detected neutrals we model their propagation into the plasma column for the experimental scenario using an implementation of the Kinetic Transport Code KN1D ([2],[3]). Although the geometry is slab-like it remains valid for plasma radii inside the SOL.

Simulation of atomic neutral profile and charge exchange flux

KN1D calculates, for thermal and stationary plasmas, the neutral atomic and molecular profiles (for deuterium see figure 5) based on provided profiles of $n_e(s)$, $T_e(s)$ and $T_i(s)$ mapped to the CNPA chord length s (see figure 4) together with the molecular neutral pressure at the wall ($p_{D_2^0}(r=a)$ for deuterium). This last parameter is not measured, but since its value is linear in the resulting neutral profiles it may be subsequently adjusted to achieve agreement of the modeled neutral particle flux

$$F^{CX}_{j,sim}(E_j)dE_j = \mu_j(A\Omega)\int_{\rho_{a_{HFS}}}^{\rho_{a_{LFS}}} \varepsilon\left(\rho,E_j\right)d\rho \qquad (3)$$

with the CNPA measurement $F^{CX}_{j,CNPA}$ (channeltron of energy E_j, energy window width dE_j, detection efficiency μ_j and throughput $A\Omega$). The relative error χ between measured and simulated F^{CX} is shown in figure 6. For this discharge, the best fit was obtained with $p_{D_2^0}(r=a)$ = 0.57 mTorr (×).

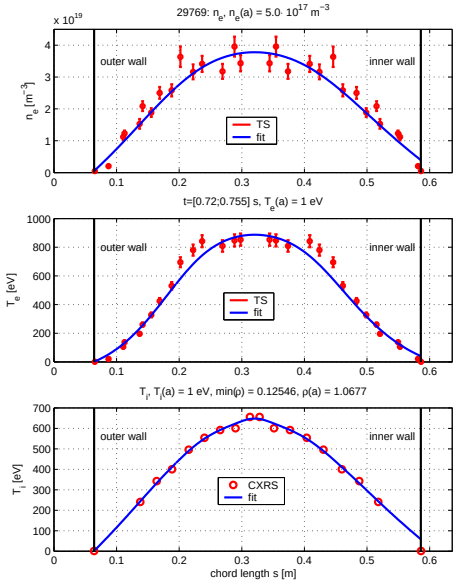

Figure 4: Plasma input profiles against CNPA chord coordinate. Diagnostics measurements (○) and fitted profiles (—) for n_e (top), T_e (middle) and T_i (bottom).

The linearity of the CX spectrum with the neutral wall pressure is illustrated with a KN1D execution with the same conditions but $p_{D_2^0}(r=a)$ increased (+) and decreased (∗) by 30 % respectively (figure 6).

The CXRS ion temperature profile is often taken over a distinct time interval (for this example at the end of the discharge), so a small correction factor, constant over the profile, is used to scale the temperature for the considered interval. Ion temperature changes lead to a positive (negative) slope in the relative error χ when the temperature is increased □ (decreased ⊙).

In ohmic discharges the generation of (fast) neutrals in the center of the tokamak is small (figure 5) and the majority of the neutrals are re-ionised on their way out of the plasma. Figure 4 shows only the deuterium channels 1 - 9 (E = 500 .. 6'500 eV) where the poisson error (◊) of the counting statistics of the CNPA is below 50 %. For this energy interval the simulation recovers the experimental CX flux with a mismatch < ∼10 %.

Recovery of the neutral birth place and ion temperature profile estimation

With the simulated atomic neutral profile, the neutral emissivity may now be calculated (equation 2), shown in figure 7. Even if, locally, the ions D^+ have a broad energy distribution characterised by the local temperature, the maxima of the neutral emissivities are sufficiently separated in space for the CNPA channel energies.

The width of the CNPA energy channels can be as large as 70 % (for E_H^0 = 500 eV) so the maximum of the incident particle distribution normally occurs at an energy lower than the channel centre E^0 (the CX-spectrum decreases with energy, see figure 3), depending on the local ion temperature. Figure 8 shows the correction for hydrogen channel 5 (E_H^0 = 4 keV) obtained from the convolution (–) of the simulated flux spectrum (–) with the instrumental function (–) showing that particles of energy E = 3850 eV are dominating the CX spectrum for this channel. This correction was performed for all the channels of figure 7, with the effect that the birth positions are shifted outwards.

We may now proceed to link the radial origin of the neutrals to their temperature upon neutralisation. Figure 7 shows that the radial coverage of channels 4 (H) / 16 (D) and 5 (H) / 18 (D) are

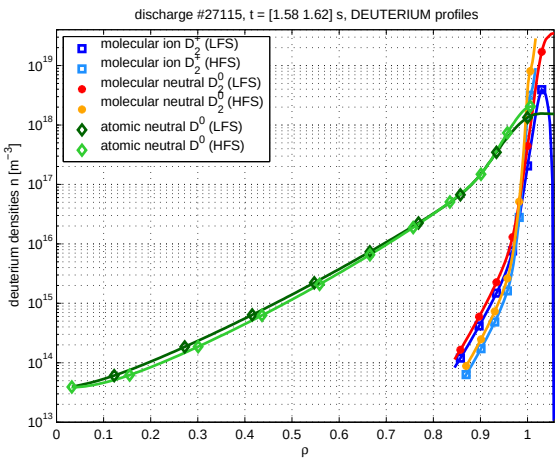

Figure 5: Simulated profiles •• neutral molecular D_2^0, □ □ molecular ion D_2^+ ◊◊ atomic neutral D^0 densities.

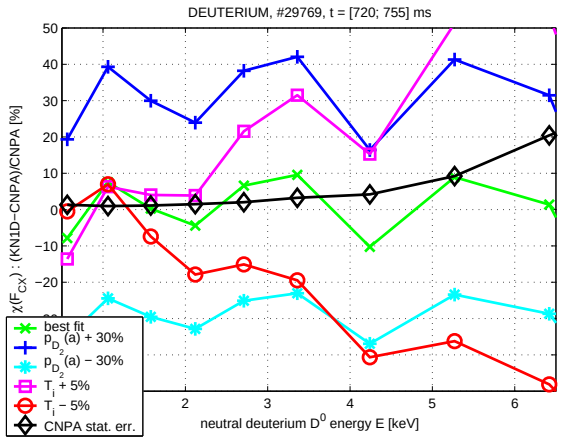

Figure 6: Relative fit error. Best fit for $p_{D_2^0}(r=a)$ = 0.57 mTorr and $T_i = T_{i,C}^{CXRS}$ (×), $p(a) \pm 30\%$ (+, •) and $T_i \pm 5\%$ (□, ⊙)

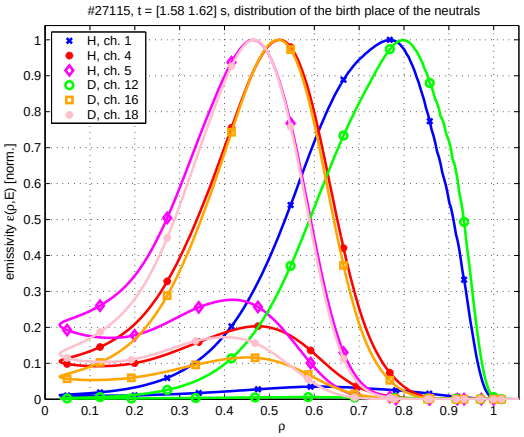

Figure 7: Normalised neutral H and D emissivities $\varepsilon(\rho, E)$ for some of the CNPA channel energies. Per energy, there is a curve for the LFS (upper) and HFS (lower).

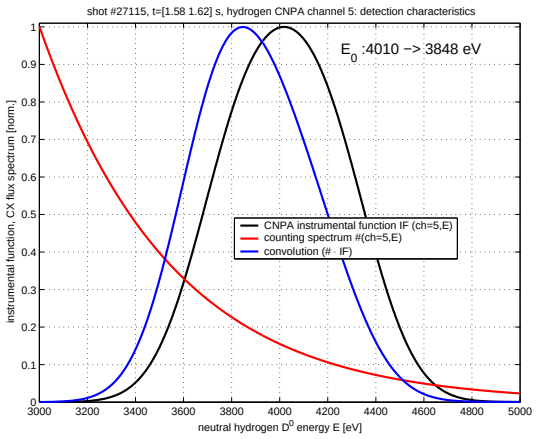

Figure 8: The convolution of the count spectrum for CNPA channel 5 (—) with the instrumental function (—) lowers the energy of the maximu m of counted particles by 5 % (—).

approximately identical. The fitted slope of the CX spectrum with equation 1 should therefore provide a radially restricted measurement of the hydrogen and deuterium ion temperature. The measured (⊙,⊙) and simulated (–,–) CX spectrum, a fit to channels 4 & 5 (H, –) and 16-18 (D, –) are shown in figure 3. From the mean value theorem, the slope of the fit that matches the simulated spectrum at some median energy E^* between the channel energies is used for the fit. Here $E^* \approx 3.5$ keV whose maximum contribution to the CX flux comes from $\rho = 0.5$ for both species. The fits give $T_{i,H(4:5)}^{CNPA} = 480$ eV and $T_{i,D(16:18)}^{CNPA} = 460$ eV, only $> \sim 10$ % from the measured carbon temperature $T_{i,C}^{CXRS}(\rho = 0.5) = 450$ eV. All the ion temperatures are close which is to be expected since the ion thermalisation time is ∼0.5 ms for this discharge which justifies the use of the CXRS profile as hydrogenic ion temperature in the input of KN1D. It should be noted that the carbon ion temperatures for KN1D were adjusted to reduce the mismatch between simulation and experiment (see figure 6) and that this correction is generally in agreement with the differences among the different ion temperatures.

The recovery procedure was applied to all neighboring channel pairs for a plasma axis moving from $z = 23$ cm to $z = 3$ cm (figure 1) to reconstruct the CNPA ion temperature profile, shown in figure 2 (circles), together with the CXRS measurement (squares) for different time intervals. For $t = 1.525$ s, the fitted CXRS profile is also plotted for comparison (–) and shows agreement within the error bars of the CNPA measurement. The horizontal error bars indicate the birthplace of 50 % of the detected neutrals.

This work was partly funded by the Fonds National Suisse de la Recherche Scientifique

References

[1] F. V. Chernyshev et al., Inst. Exp. Tech., **47** (2004) 214.

[2] A. N. Karpushov et al., 30^{th} EPS Conf. PCCF, London, P-2.152, ECA **28G** (2004)

[3] B. LaBombard, KN1D, PSFC/RR-01-9, MIT, Cambridge (2001).